

## Optical rotation inversion of porphyrin–DNA complexes

Chikako Takatoh,<sup>b</sup> Takuya Matsumoto,<sup>a,\*</sup> Tomoji Kawai,<sup>a,\*</sup> Takayuki Shitoh<sup>b</sup> and Kazuyoshi Takeda<sup>b</sup>

<sup>a</sup>*Institute of Scientific and Industrial Research, Osaka University, 8-1 Mihogaoka, Ibaraki, Osaka 567-0047, Japan*

<sup>b</sup>*Ebara Research Co. Ltd, 4-2-1 Honfujisawa, Fujisawa, Kanagawa 251-8502, Japan*

Received 11 October 2005; revised 9 November 2005; accepted 10 November 2005

Available online 28 November 2005

**Abstract**—A porphyrin–DNA complex in which helical porphyrin assemblies were stacked as  $\pi$ -stacked aggregates on a DNA scaffold was found. The complex indicates the inversions of optical rotation by only the control of ionic equilibrium without any structural changes of DNA scaffold.

© 2005 Elsevier Ltd. All rights reserved.

Chiral architecture has been investigated using a variety of approaches, including the synthesis of helical polymers and the self-assembly of synthesized molecules and proteins.<sup>1,2</sup> Synthetic approaches for covalently attaching dyes to chiral structures have been developed for the generation of optically active materials with both photonic and photoelectronic functionalities. Recently, DNA, a chiral and readily available molecule, has been used to create optically active materials.

The binding interactions between functional molecules and DNA can be divided into five categories: covalent bonds,<sup>3</sup> intercalation,<sup>4</sup> inclusion in wide and narrow grooves,<sup>5,6</sup> and ionic bonds.<sup>7</sup> Ionic bonding at the DNA backbone allows supramolecular reactions in aqueous solution, while maintaining the natural form of DNA. This also allows high-density integration, wherein one functional cation is bound to each phosphate group per base pair. Here, we report a new porphyrin–DNA complex in which helical porphyrin assemblies are stacked on a DNA scaffold by control of the ionic equilibrium. It is found that optical rotation change of porphyrin  $\pi$ -stacked aggregates<sup>8</sup> are induced by only the control of ionic equilibrium without any structural changes of DNA scaffold. This is a new class of optical rotation tunable porphyrin architecture distin-

guished from previous studies using single-stranded DNAs or pigment-proteins as scaffolds.<sup>9</sup>

Ionic assembly employing a DNA backbone requires that porphyrin (i) contains outward cationic groups for binding of DNA phosphate; (ii) is prevented from intercalating into the base stacking of the DNA double helix by steric hindrance; and (iii) allows  $\pi$ -stacked aggregation. These requirements are satisfied by 5,10,15,20-tetrakis-4-trimethylammonio-phenylporphyrin-tetraluene-4-sulfonate (TMAP; Fig. 1), which bears four phenyl groups attached to each quaternary ammonium cation at the meso position of a porphyrin ring. In fact, a previous study of Ref. 5 reported that the TMAP is prevented completely from the intercalation by a steric effect. The perpendicular configuration between phenyl and heme planes is also supported by density function theory (DFT; B3LYP/6-31G\*) calculation.

In the present study, we used poly(dA)/poly(dT) DNA for complex formation with TMAP. The porphyrin–DNA complexes were formed in aqueous solution at a variety of concentration ratios ( $R$ ):<sup>5</sup>

$$R = [\text{porphyrin}]/[\text{PO}_4^-]$$

Because TMAP is a tetravalent cation, the TMAP–DNA complex precipitates at  $R = 1/4$  of the isoelectric concentration ratio.

To examine the formation of TMAP–DNA complexes, we obtained UV/vis absorption spectra for various  $R$

**Keywords:** Optical rotation;  $\pi$ -stacking.

\* Corresponding authors. Tel.: +81 6 6879 4288; fax: +81 6 6875 2440; e-mail addresses: [takatoh.chikako@er.ebara.com](mailto:takatoh.chikako@er.ebara.com); [matsumoto@sanken.osaka-u.ac.jp](mailto:matsumoto@sanken.osaka-u.ac.jp); [kawai@sanken.osaka-u.ac.jp](mailto:kawai@sanken.osaka-u.ac.jp)

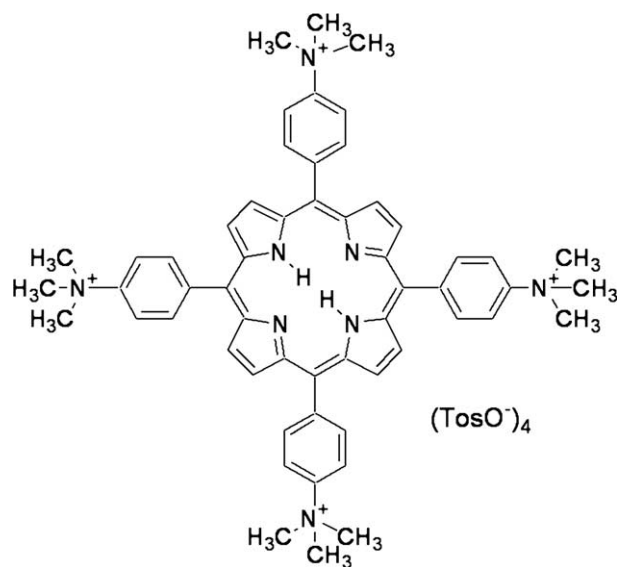


**Figure 1.** Molecular structure of TMAP.

values generated by varying the DNA concentrations at a constant concentration of TMAP. **Figure 2a** shows the absorption spectra of TMAP for the Soret band region, and **Figure 3** indicates the change of absorbance ratio of the peaks deconvoluted from the spectra of **Figure 2a** as a function of the DNA concentration. An aqueous solution of TMAP without DNA showed only a peak at 411 nm with a 12 nm half width. As the DNA concentration was increased to  $1/R = 4$ , the absorbance of the peak decreased remarkably. This reduction is caused by the formation of an insoluble salt of DNA and TMAP. With further increases in the DNA concentration, the TMAP–DNA complex becomes soluble again

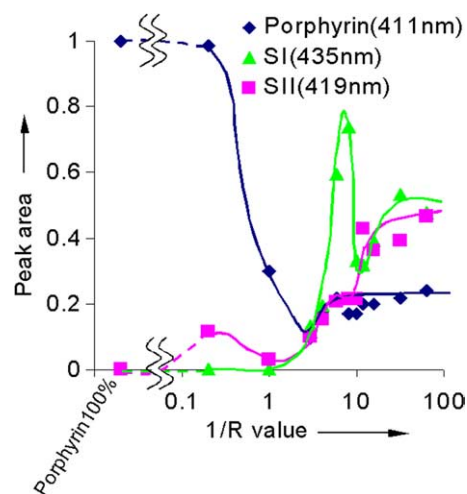


**Figure 3.** Absorbance peak areas. Absorbance peak areas for SI (435 nm), SII (419 nm), and free TMAP (411 nm) as a function of the concentration ratio,  $R$ . The plots were normalized by the absorbance of free TMAP at 419 nm.

due to the presence of excess phosphate groups. Concurrently, a red-shifted and broadened peak at 435 nm with a 17 nm half width appeared and reached a maximum absorbance at  $1/R = 8$  with further increases in the DNA concentration (increased  $1/R$ ). This peak (SI) is accompanied by a shoulder at 420 nm with a 14-nm half width (SII). As the concentration of DNA was increased, the SII shoulder became a well-resolved peak and the spectral weight moved rapidly from SI to SII. This steep rise and fall suggest that the SI peak is formed only when there is ionic equilibrium and  $\pi$ -stacking between TMAPs. Appearance of these two red-shifted and broadened peaks suggests the presence of a dipole

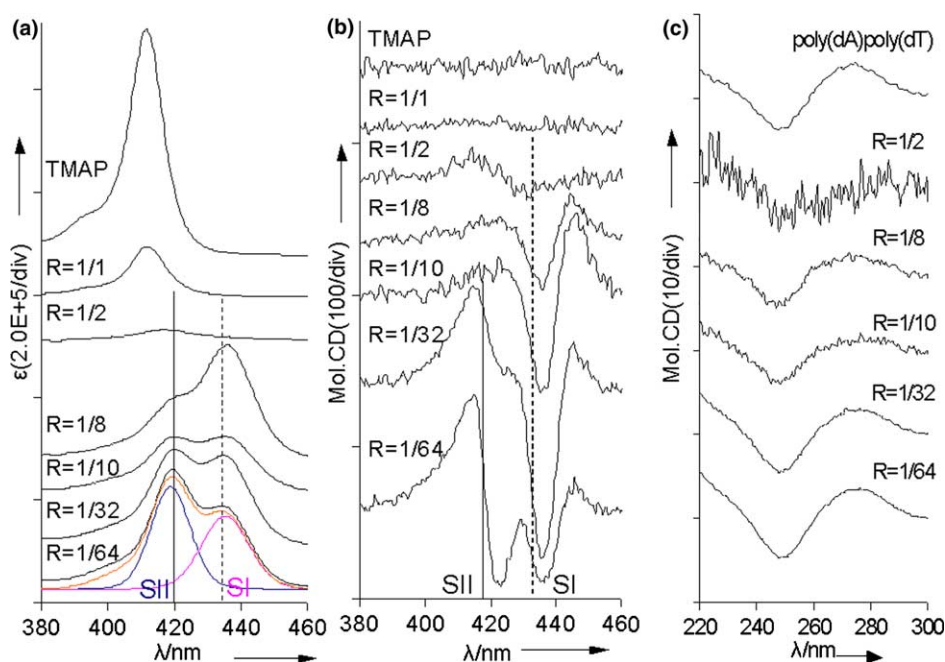


**Figure 2.** Absorption and CD spectra. The spectra for the TMAP–DNA complex in aqueous solution. (a) Absorption spectra for the Soret band, (b) CD for the Soret band, and (c) CD spectra for DNA base absorption band at various concentration ratios ( $R = 1/1, 1/2, 1/8, 1/10, 1/32, \text{ and } 1/64$ ).

coupling interaction derived from the formation of TMAP–DNA complexes. Because the steric effect of TMAP inhibits it from intercalating into the DNA double helix, the dipole coupling interaction can be attributed to head-to-tail aggregation<sup>8</sup> of TMAPs bound to the DNA backbone. According to the theory developed by Kasha,<sup>10</sup> the large red-shift suggests that the intermolecular distance between TMAPs of SI is closer than that of SII. Furthermore, the considerable broadening of the SI peak also reflects a strong intermolecular interaction.

Figure 2b shows the circular dichroism (CD) spectra corresponding to the visible absorption spectra in Figure 2a. Without DNA (TMAP alone), there was no CD signal. Upon addition of DNA, CD signals for TMAP appeared at the wavelengths of the absorption spectra. This indicates the formation of a chiral porphyrin–DNA complex. The SI peak is dextrorotatory, corresponding to the optical rotation of the DNA double helix. In contrast, the SII peak is levorotatory.

To clarify whether the optical rotation inversion is induced by a DNA structural change, we examined the CD spectrum around 260 nm. This spectrum shows the absorption of stacked nucleic bases, and allows determination of the structure of the DNA double helix. The CD spectrum at  $R$  values between 1/2 and 1/64 for the DNA region in Figure 2c (which corresponds to the portion of the CD that dramatically changed for TMAP) is identical to the reference spectrum for poly-(dA)/poly(dT) in the absence of TMAP. This indicates that the conversion from SI to SII is unrelated to a structural change in the DNA double helix.

We next investigated the effect of adding NaCl to the TMAP–DNA solution ( $1/R = 10$ ) to examine the stability of SI to structural changes in the DNA double helix. At 0.05–25 mM NaCl, the CD spectra at 260 nm indicated a partial change of the DNA double helix from a B form to an A form (Fig. 4a).<sup>11</sup> Concurrently, the CD signal for TMAP changed from SI to SII

(Fig. 4b). Despite the structural change in the DNA, the CD behavior of the TMAP peaks was similar to that obtained by varying  $R$  while maintaining the B form of the DNA.

We also investigated the effect of pH by UV/vis and CD spectroscopy. The pH was varied from 7 to 9 by adding Tris-EDTA (TE) or Tris (TR) buffers (data not shown). Similar to NaCl, the addition of TE or TR induced partial changes in the DNA structure from the B to the A form and converted the TMAP structure from SI to SII. These findings suggest that, complex formation with SI is unstable or unfavorable under the ionic conditions needed to stabilize the A form of the DNA.

The aggregation of TMAP in the TMAP–DNA complex is supported by not only spectroscopic analysis but also by atomic force microscopy (AFM). Figure 5 shows AFM images of TMAP–DNA complexes (panel a) and DNA without TMAP (panel b). The height of the TMAP–DNA complex and DNA without TMAP are approximately 0.5 and 0.3 nm, respectively. The high protrusion of the TMAP–DNA complex implies that TMAP bound to the outside of the DNA helix by ionic

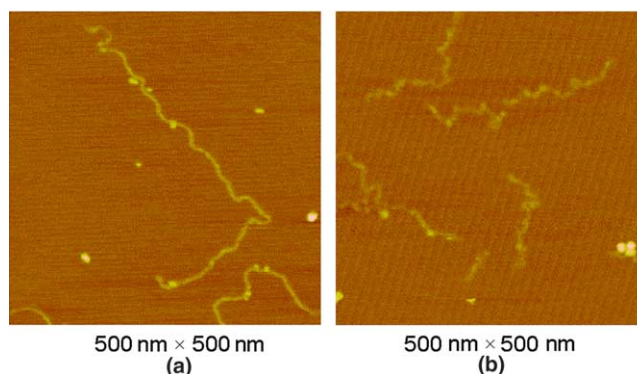


Figure 5. AFM images. The image of (a) TMAP–DNA complex and (b) pure DNA on a mica substrate. Images were taken under tapping mode in air.

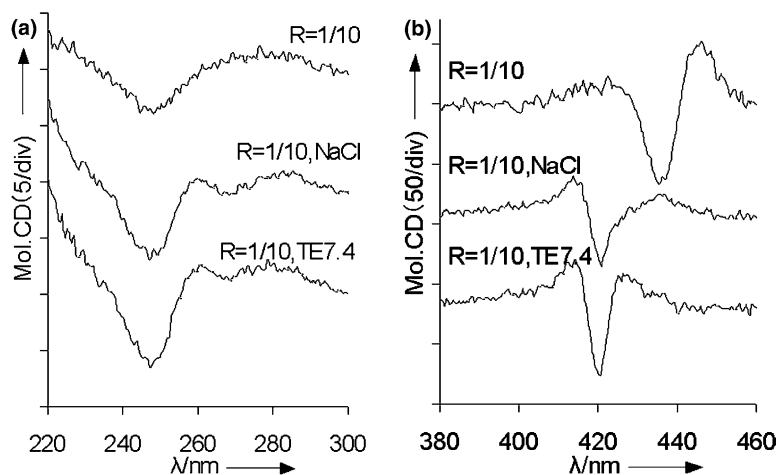
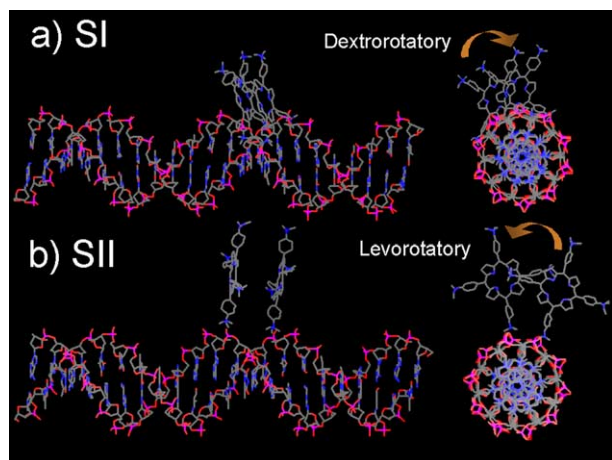


Figure 4. CD spectra. The spectra for (a) the DNA base absorption band and (b) the Soret band for the TMAP–DNA complex at  $R = 1/10$  with no added NaCl or buffer or with 25 mM NaCl or TE (pH 7.4).



**Figure 6.** Structural model. The model for the TMAP–DNA complex. (a) SI and (b) SII.

interactions with DNA backbone phosphates. Furthermore, the morphology of the TMAP–DNA strands was very different from that of the TMAP-free DNA strands. The TMAP–DNA strands behaved like a rigid rod, whereas the DNA without TMAP showed random walk behavior. The rigid rod behavior indicates that aggregation of TMAP reduces the flexibility of the TMAP–DNA complex.

Figure 6 shows possible models for SI and SII based on our findings. The CD spectrum for SI is dextrorotatory, corresponding to the DNA double helix. Therefore, the alignment of the TMAP molecule along the DNA strands is a reasonable explanation for our CD spectra. Moreover, the large red shift in the absorbance peaks of SI indicates the presence of strong dipole coupling for  $\pi$ -stacked aggregated porphyrins with short distance. Furthermore, TMAP aggregation is also suggested by rigid rod behavior in AFM images. To satisfy these characteristics of TMAP/DNA complex, we propose a structural model for SI complex as shown in Figure 6a. In this model, TMAP straddles a vice-groove, forming a bridge between two ionic bonds of neighboring ammonium ions from a TMAP molecule and the phosphate anions of two different backbones of a double-stranded DNA molecule. In this proposed structure, the distance between the two phosphate anions of the two DNA strands is equal to that between the two neighboring ammonium ions in TMAP. Thus, it is reasonable to assume that TMAP stacks tightly and with a dextrorotatory structure.

In contrast, SII, which is levorotatory, suggests the presence of TMAP aggregates formed over the groove of the

DNA double helix. The nearest two TMAP molecules straddling the vice-groove can form a head-to-tail TMAP pair with a distance of 1.17 nm. In this case, the stereochemistry indicated that the two TMAP molecules are oriented opposite to the DNA helix.

In conclusion, we identified a novel TMAP–DNA complex (SI) indicating the large red-shift (435 nm) of the absorption peak in the Soret band. Without any structural change of DNA scaffold, a dramatic optical rotation inversion of porphyrin  $\pi$ -stacked aggregates occurred when this was changed to the well-known SII complex by alteration of the concentration ratio. This is similar to a phase transition in porphyrin aggregation with an inversion of optical rotation on a fixed DNA scaffold.

### Acknowledgements

We thank Dr. Tetsuo Osa of Tohoku University for helpful discussions and advice.

### References and notes

- Okano, T.; Okamoto, Y. *Chem. Rev.* **2001**, *101*, 4013; Cornelissen, J. J. M.; Rowan, A. E.; Nolte, R. J. M.; Sommerdijk, N. A. J. M. *Chem. Rev.* **2001**, *101*, 4039; Green, M. M.; Cheon, K.; Yun, S.; Park, J.; Swansburg, S.; Liu, W. *Acc. Chem. Res.* **2001**, *304*, 672.
- Takahashi, R.; Kobuke, Y. *J. Am. Chem. Soc.* **2003**, *125*, 2372; Witte, P. A. J.; Castriciano, M.; Cornelissen, J. J. L. M.; Scolaro, L. M.; Nolte, R. J. M.; Rowan, A. E. *Chem. Eur. J.* **2003**, *9*, 1775.
- Balaz, M.; Holmes, A. E.; Benedetti, M.; Rodrigues, P.; Berova, N. *J. Am. Chem. Soc.* **2005**, *127*, 4172.
- Lang, J.; Liu, M. *J. Phys. Chem. B.* **1999**, *103*, 11393.
- McClure, J. E.; Baudouin, L. *Biopolymers* **1997**, *42*, 203; Carvlin, M. C.; Fiel, R. J. *Nucleic Acids Res.* **1983**, *11*, 6121.
- Young, L.; Jin, K.; Tae, C.; Rita, S.; Seog, K. K. *J. Am. Chem. Soc.* **2003**, *125*, 8106; Scolaro, L. M.; Romeo, A.; Pasternack, R. F. *J. Am. Chem. Soc.* **2004**, *126*, 7178.
- Nakayama, H.; Ohno, H.; Okahata, Y. *Chem. Commun.* **2001**, *22*, 2300.
- Jelly, E. E. *Nature* **1936**, *138*, 1009; Scheibe, G. *Angew. Chem.* **1936**, *49*, 563.
- Pasternack, R. F.; Gurrieri, S.; Lauceri, R.; Purrello, R. *Inorg. Chim. Acta* **1996**, *246*, 7; Pancoska, P.; Urbanova, M.; Bednarova, L.; Vacek, K.; Paschenko, V. Z.; Vasiliev, S.; Malon, P.; Kral, M. *Chem. Phys.* **1990**, *147*, 401.
- Kasha, L.; Rawls, H. R.; BL-Bayoumi, M. A. *Pure Appl. Chem.* **1965**, *11*, 371.
- Ivanov, V. I.; Minchenkova, L. E.; Schyolkina, A. K.; Poletayev, A. I. *Biopolymers* **1973**, *12*, 89.